Sulfate as a Synergistic Anion Facilitating Iron Binding by the Bacterial Transferrin FbpA: The Origins and Effects of Anion Promiscuity

4 AUTHORS, INCLUDING:

Timothy Mietzner
Lake Erie College of Osteopathic Medicine

80 PUBLICATIONS **2,491** CITATIONS

SEE PROFILE

Sulfate as a Synergistic Anion Facilitating Iron Binding by the Bacterial Transferrin FbpA: The Origins and Effects of Anion Promiscuity

J. J. Heymann,[†] K. D. Weaver,[†] T. A. Mietzner,[‡] and A. L. Crumbliss*,[†]

Contribution from the Department of Chemistry, Duke University, Durham, North Carolina 27708-0346, and Department of Molecular Genetics and Biochemistry, University of Pittsburgh School of Medicine, Pittsburgh, Pennsylvania 15261

Received February 8, 2007; E-mail: alvin.crumbliss@duke.edu

Abstract: The ferric binding protein, FbpA, has been demonstrated to facilitate the transport of naked Fe^{3+} across the periplasmic space of several Gram-negative bacteria. The sequestration of iron by FbpA is facilitated by the presence of a synergistic anion, such as phosphate or sulfate. Here we report the sequestration of Fe^{3+} by FbpA in the presence of sulfate, at an assumed periplasmic pH of 6.5 to form FeFbpA-SO_4 with $K'_{eff} = 1.7 \times 10^{16}$ M^{-1} (at 20 °C, 50 mM MES, 200 mM KCl). The iron affinity of the FeFbpA-SO_4 protein assembly is 2 orders of magnitude lower than when bound with phosphate and is the lowest of any of the FeFbpA-X assemblies yet reported. Iron reduction at the cytosolic membrane receptor may be an essential aspect of the periplasmic iron-transport process, and with an $E_{1/2}$ of -158 mV (NHE), FeFbpA-SO_4 is the most easily reduced of all FeFbpA-X assemblies yet studied. The variation of FeFbpA-X assembly stability (K_{eff}) and ease of reduction ($E_{1/2}$) with differing synergistic anions X^{n-} are correlated over a range of 14 kJ, suggesting that the variations in redox potentials are due to stabilization of Fe^{3+} in FeFbpA-X by X^{n-}. Anion promiscuity of FbpA in the diverse composition of the periplasmic space is illustrated by the ex vivo exchange kinetics of FeFbpA-SO_4 with phosphate and arsenate, where first-order kinetics with respect to FeFbpA-SO_4 ($k = 30$ s^{-1}) are observed at pH 6.5, independent of entering anion concentration and identity. Anion lability and influence on the iron affinity and reduction potential for FeFbpA-X support the hypothesis that synergistic anion exchange may be an important regulator in iron delivery to the cytosol. This structural and thermodynamic analysis of anion binding in FeFbpA-X provides additional insight into anion promiscuity and importance.

Introduction

Iron is an essential element for nearly every living organism. The survival of each cell is dependent on its ability to acquire and sustain a necessary quantity of this transition metal.[1] However, the iron acquisition processes of even the most rudimentary organism are quite complex, with strict requirements due to the paradoxical properties of iron in biology: necessity, insolubility, and toxicity.[2] While iron is essential to sustain life, under certain conditions the metal can act as a redox center, facilitating the production of harmful reactive oxygen species through Fenton chemistry and the Haber−Weiss cycle.[1] Also, while iron is the second most abundant metal on the earth's surface, it predominantly exists as biologically unavailable iron hydroxide polymers, requiring that microorganisms develop specialized means of acquiring sufficient concentrations of this element.[2]

For pathogenic bacteria, the ability to successfully acquire iron from the environment is directly related to virulence.[3−5]

There are two common means of microbial iron uptake. The first is accomplished through the synthesis of a low-molecular weight organic chelator molecule, known as a siderophore, which is released to the environment to selectively sequester iron and return to the microbial colony.[6−11] The second method of iron acquisition is a protein-mediated system.[3] In either case, it is critical for bacteria to gain control of the first-coordination shell of iron to inhibit its toxic effects, including the synthesis of reactive oxygen species and resulting oxidative damage. Therefore, iron acquisition is not just simple recognition and

[†] Duke University.
[‡] University of Pittsburgh School of Medicine.
(1) Crichton, R. R. *Inorganic Biochemistry of Iron Metabolism: From Molecular Mechanism to Clinical Consequences*, 2nd ed.; Wiley: New York, 2001.
(2) Crosa, J. H.; Mey, A. R.; Payne, S. M. *Iron Transport in Bacteria*; ASM Press: Washington DC, 2004.

(3) Mietzner, T. A.; Tencza, S. B.; Adhikari, P.; Vaughan, K. G.; Nowalk, A. J. In *Current Topics Microbiology and Immunology*; Vogt, P. K., Mahan, M. J., Eds.; Springer: Berlin, 1998; Vol. 225, pp 113−35.
(4) Sritharan, M. *World J. Microbiol. Biotechnol.* **2000**, *16*, 769−80.
(5) Clarke, T. E.; Tari, L. W.; Vogel, H. J. *Curr. Top. Med. Chem.* **2001**, *1*, 7−30.
(6) Winkelmann, G.; van der Helm, D.; Neilands, J. B. *Iron Transport in Microbes, Plants and Animals*; VCH Publishers: New York, 1987.
(7) Matzanke, B. F.; Muller-Matzanke, G.; Raymond, K. In *Iron Carriers and Iron Proteins*; Loehr, T. M., Ed.; VCH Publishers: New York, 1989; pp 1−22.
(8) Albrecht-Gary, A.-M.; Crumbliss, A. L. In *Metal Ions in Biological Systems*; Sigel, A., Sigel, H., Eds.; Marcel Dekker: New York, 1998; pp 239−327.
(9) Boukhalfa, H.; Crumbliss, A. L. *BioMetals* **2002**, *15*, 325−339.
(10) Dhungana, S.; Crumbliss, A. L. *Geomicrobiol. J.* **2005**, *22*, 87−98.
(11) Raymond, K. N.; Dertz, E. A. In *Iron Transport in Bacteria*; Crosa, J. H., Mey, A. R., Payne, S. M., Eds.; ASM Press: Washington DC, 2004; pp 3−17.

transport at the bacterial cell surface; it is also an issue of "iron-management".

Certain Gram-negative bacteria, including the genera *Neisseria* and *Haemophilus*, express surface receptors specific for host iron-transport proteins (e.g., lactoferrin and transferrin), which bind the host iron carrier and pilfer the precious metallic cargo.[3,5] A series of proteins mediate the transfer of the iron from these host iron binding proteins into the bacterial cytoplasm.[12,13] In these cases, a single periplasmic iron binding protein, ferric binding protein (FbpA), designated hFbpA (HitA) in *Haemophilus influenzae* and nFbpA (FbpA) in *Neisseria gonorrheae*,[14] effectively mediates non-heme iron transport from the inside of the outer membrane to the outside of the inner membrane.[3,5,16−19] As the only means of shuttling iron across the periplasmic space, FbpA plays a pivotal role in the iron-uptake process of these pathogens, perhaps as the rate-limiting step in bacterial iron acquisition.[3]

FbpA is a member of the transferrin superfamily of proteins that traces its ancestry to an anion binding protein.[20] FbpA is referred to as bacterial transferrin, a title attributed to both functional and structural similarities to mammalian transferrin.[20−23] This bacterial transferrin acts as a transport protein, shuttling iron between membrane receptors, analogous to its human transferrin (*h*Tf) counterpart. Structurally, Fbp from *H. influenzae* and *N. gonorrheae* contains a single functional site and exhibits protein folding similar to a single lobe of the bilobal *h*Tf. In all three proteins, iron is hexa-coordinate, bound by two tyrosines, a histidine, and a carboxylic acid, provided by either aspartate (*h*Tf) or glutamate (Fbp), with the final two coordination sites occupied by an exogenous anion, bidentate carbonate for *h*Tf[23,24] and, from the reported crystal structure, a monodentate phosphate anion and water for FbpA.[20] The anion- and iron binding sites are illustrated in Figure 1 for apo-HitA and holo-FbpA, relating both Fbp and Tf to the anion binding superfamily of proteins.[20]

A synergistic anion derived from the exogenous environment is essential for both Fbp and Tf to facilitate tight iron binding. In FbpA, numerous anions have been found to serve the essential function of the synergistic anion in vitro.[25−28] These anions are

(12) Cornelissen, C. N.; Sparling, P. F. In *Iron Transport in Bacteria*, Crosa, J. H., Ed. ASM Press: Washington D.C., 2004; pp 256−272.

(13) Morton, D. J.; Stull, T. L. In *Iron Transport in Bacteria*; Crosa, J. H., Ed.; ASM Press: Washington DC, 2004; pp 273−292.

(14) There is 71% amino acid sequence fidelity between *Neisseria gonorrhoeae* and *Haemophilus influenzae*.[15]

(15) Macromolecular Structure Database (MSD); Structural alignment results via European Molecular Biology Laboratory−European Bioinformatics Institute (EMBL-EBI), query pdb entry 1d9y (holo-FbpA), target pdb entry 1mrp (holo-HitA).

(16) Chin, N.; Frey, J.; Chang, C.-F.; Chang, Y.-F. *FEMS Microbiol. Lett.* **1996**, *143*, 1−6.

(17) Saken, E.; Rakin, A.; Heesemann, J. *Int. J. Med. Microbiol.* **2000**, *290*, 51−60.

(18) Gong, S.; Bearden, S. W.; Geoffroy, V. A.; Fetherston, J. D.; Perry, R. D. *Infect. Immun.* **2001**, *69*, 2829−2837.

(19) Adhikari, P.; Berish, S. A.; Nowalk, A. J.; Veraldi, K. L.; Morse, S. A.; Mietzner, T. A. *J. Bacteriol.* **1996**, *178*, 2145−2149.

(20) Bruns, C. M.; Nowalk, A. J.; Arvai, A. S.; McTigue, M. A.; Vaughan, K. G.; Mietzner, T. A.; McRee, D. E. *Nat. Struct. Biol.* **1997**, *4*, 919−924.

(21) Bruns, C. M.; Anderson, D. A.; Vaughan, K. G.; Williams, P. A.; Nowalk, A. J.; McRee, D. E.; Mietzner, T. A. *Biochemistry* **2001**, *40*, 15631−15637.

(22) MacGillivray, R. T. A.; Moore, S. A.; Chen, J.; Anderson, B. F.; Baker, H.; Luo, Y.; Bewley, M.; Smith, C. A.; Murphy, M. E. P.; Wang, Y.; Mason, A. B.; Woodworth, R. C.; Brayer, G. D.; Baker, E. N. *Biochemistry* **1998**, *37*, 7919−7928.

(23) Bailey, S.; Evans, R. W.; Garratt, R. C.; Gorinsky, B.; Hasnain, S.; Horsburgh, C.; Jhoti, H.; Lindley, P. F.; Mydin, A.; Sarra, R.; Watson, J. L. *Biochemistry* **1988**, *27*, 5804−5812.

(24) Baker, H. M.; Anderson, B. F.; Brodie, A. M.; Shongwe, M. S.; Smith, C. A.; Baker, E. N. *Biochemistry* **1996**, *35*, 9007−9013.
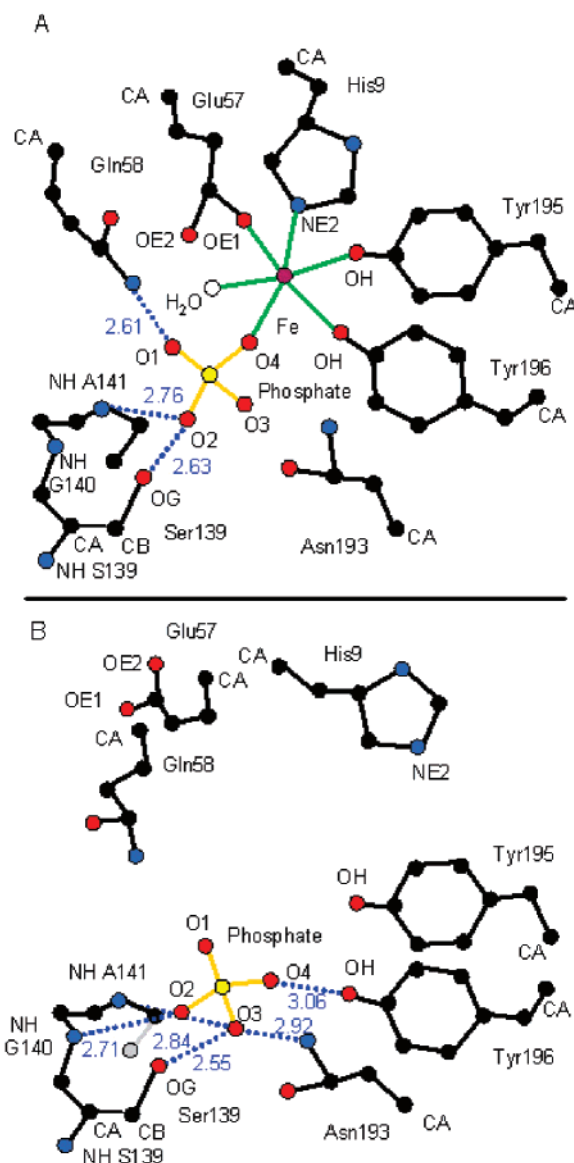
Figure 1. Ligand plots developed using kinemages displaying ferric binding protein, designated HitA (hFbpA) in *H. influenzae* and FbpA (nFbpA) in *N. gonorrheae*. The ligand interactions for FeFbpA-PO$_4$ and apo-HitA are shown between phosphate, iron, and protein. (A) Ligand interaction map using holo-FbpA backbone. The holo interactions for phosphate are Ser139, Ala141 amide N, and Gln58. The holo interactions for iron are water, Glu57, His9, Tyr195, Tyr196, and phosphate. (B) Ligand interaction map using apo-HitA backbone. The apo interactions for phosphate are Ser139, Gly140 amide N, Ala141 amide N, Tyr196, and Asn193. Hydrogen bonds are shown by dashed blue lines with the bond length (Å) printed in blue. Coordinate files: 1D9Y.pdb[38] and 1D9V.pdb.[21]

readily exchangeable upon in vitro manipulation and, at pH 6.5, modulate the iron affinity of the FeFbpA-X assembly over the log K'_{eff} range 17−18 and the Fe^{3+}/Fe^{2+} redox potential over the range −300 to −180 mV (NHE).[25,26,29] Given the diverse composition of the periplasm,[30] this synergistic anion promiscu-

(25) Taboy, C. H.; Vaughan, K. G.; Mietzner, T. A.; Aisen, P.; Crumbliss, A. L. *J. Biol. Chem.* **2001**, *276*, 2719−2724.

(26) Dhungana, S.; Taboy, C. H.; Anderson, D. A.; Vaughan, K. G.; Aisen, P.; Mietzner, T. A.; Crumbliss, A. L. *Proc. Natl. Acad. Sci. U.S.A.* **2003**, *100*, 3659−3664.

(27) Roulhac, P. L.; Powell, K. D.; Dhungana, S.; Weaver, K. D.; Mietzner, T. A.; Crumbliss, A. L.; Fitzgerald, M. C. *Biochemistry.* **2004**, *43*, 15767−15774.

(28) Guo, M.; Harvey, I.; Yang, W.; Coghill, L.; Campopiano, D. J.; Parkinson, J. A.; MacGillivray, R. T. A.; Harris, W. R.; Sadler, P. J. *J. Biol. Chem.* **2003**, *278*, 2490−2502.

ity may be biologically significant. Since the anion-dependent redox potentials are in the range where reduction may be driven by NADH/NADPH cofactors, a possible role for the anion has been proposed in modulating the delivery of iron to the cytosol through a redox process.[25,26] While the significance of the synergistic anion to the in vivo function of FbpA has been questioned on the basis of crystallographic interpretations of FbpA mutant data,[31] the anion-binding influence on biologically relevant physicochemical properties of FbpA in solution is clearly demonstrable. The role of the synergistic anion in vivo remains an open biological question and may be important in understanding the mechanism of iron assimilation by pathogenic bacteria utilizing FbpA orthologs.

In this work, we study both the thermodynamic and kinetic ability of sulfate to act as the synergistic anion in iron sequestration by FbpA at the periplasmic pH of 6.5.[30,32,33] By producing the least thermodynamically stable of the synergistic anion−protein assemblies, sulfate expands the range with which FbpA can modulate the ease of iron reduction simply through anion exchange. These findings have broader implications for a reductase-driven iron delivery to the cytosol[26] and expand our previous findings by demonstrating that various synergistic anions produce thermodynamically stable, kinetically labile protein assemblies. A structural analysis is described to define the role of the anion in complex stabilization and the relationship to the larger anion binding protein superfamily. In this analysis, we examine the anion influence in modulating the stability of these assemblies through iron−anion ($Fe^{3+}///X^{n-}$), protein−anion ($FbpA///X^{n-}$), and iron−protein ($Fe^{3+}///FbpA$) interactions.

Materials and Methods

Reagents. Solutions were prepared in distilled water using the highest grade of commercially available reagents. Buffer solutions of 0.05 M MES (Fisher Biotech, enzyme grade)/background electrolyte were made, with the pH adjusted to 6.5 using an Orion pH-meter model 230 with the appropriate electrolyte.

Preparation of Anion-Substituted Holo-Ferric Binding Protein, FeFbpA-X. Recombinant FbpA from *N. gonorrheae* was overexpressed in *Escherichia coli* and isolated as previously described.[34] Anion-substituted FeFbpA-X assemblies were prepared for sulfate, phosphate, and arsenate anions as follows. FeFbpA-SO₄ was prepared by the addition of 1.2 equiv of ferrous sulfate (Allied Chemical) and 10 equiv of sulfate (sodium sulfate, Fisher Scientific) to 1 equiv of apo-FbpA ([apo-FbpA] = 0.1−1.1 mM). FeFbpA-PO₄ and FeFbpA-AsO₄ were prepared by mixing 10 equiv of phosphate (potassium phosphate, monobasic, United States Biochemical) or arsenate (arsenic acid, sodium salt, ICN Biomaterials) with 1 equiv of apo-FbpA, then adding 1.2 equiv of FeCl₂ (ICN Biomedicals) while stirring gently for 30 min and then storing at 4 °C overnight. An UV−vis spectrum was taken before and after storage, with additional appropriate ferrous salt added to ensure complete Fe^{3+} loading of the protein, indicated by no changes in the

(29) Boukhalfa, H.; Anderson, D. A.; Mietzner, T. A.; Crumbliss, A. L. *J. Biol. Inorg. Chem.* **2003**, *8*, 881−892.
(30) Ferguson, S. J. In *Prokaryotic Structure and Function: A New Perspective*; 47th Symposium of the Society for General Microbiology; Mohan, S., Dow, C., Coles, J. A., Eds.; Cambridge University Press: Cambridge, 1991.
(31) Khan, A.; Shouldice, S. R.; Tari, L. W.; Schryvers, A. B. *Biochem. J.* **2007**, *403*, 43−48.
(32) The active transport of metals in Gram-negative bacteria is coupled to the electrochemical proton gradient (proton motive force) and the hydrolysis of ATP which render the periplasm acidic, thus prompting us to choose the slightly acidic pH of 6.5 for our studies.[30]
(33) Ferguson, A. D.; Deisenhofer, J. *Cell* **2004**, *116*, 15−24.
(34) Adhikari, P.; Kirby, S. D.; Nowalk, A. J.; Veraldi, K. L.; Schryvers, A. B.; Mietzner, T. A. *J. Biol. Chem.* **1995**, *270*, 25142−25149.

Table 1. Anion Binding Constants for apo-FbpA (K_d), Anion Average Charge at pH 6.5 (Z_{ave}), and Calculated Anion Hydration Enthalpies (ΔH_{hyd})

anion	K_d (mM)[a]	Z_{ave}[b]	ΔH_{hyd} (kJ mol⁻¹)[c]
sulfate	4.1 (5)[d]	−2.0	−1130
arsenate	2.1 (4)[e]	−1.4	−521
phosphate	1.6 (4)[e]	−1.4	−498
NTA	3.0 (4)[e]	−2.0	−
oxalate	0.21 (5)[e]	−2.0	−1080
citrate	0.06 (1)[e]	−2.5	−
pyrophosphate	0.018 (7)[e]	−2.8	−845

[a] Conditions: [FbpA] = 15 mM with [X^{n-}] varying from 0.5 to 100 mM, in 50 mM MES/100 mM NaCl, pH 6.5, via difference spectroscopy. Values are determined as an average of three independent experiments. Number in parentheses indicates the standard error in three independent determinations of K_d. [b] Average anion charge at pH 6.5. See Experimental Section. [c] Hydration enthalpy calculated values using eq 7. Calculated values agree with experimental values where available for sulfate and oxalate.[43,45] [d] This work. [e] Reference 47.

spectrum. The identity of the FeFbpA-X species was determined by the λ_{max} in the visible region: FeFbpA-PO₄ λ_{max} = 481 nm (ϵ_{481} = 2430 M⁻¹ cm⁻¹);[26] FeFbpA-AsO₄ λ_{max} = 476 nm (ϵ_{476} = 2280 M⁻¹ cm⁻¹);[26] FeFbpA-SO₄ λ_{max} = 495 nm (ϵ_{495} = 2460 M⁻¹ cm⁻¹).[35] Excess iron present as insoluble Fe(OH)₃ was removed by using a syringe-driven 0.45 μm filter unit (Millex, Millipore). The resulting solution was dialyzed three times against the appropriate buffer at pH 6.5 and stored at 4 °C. The final protein concentration was determined by monitoring the absorbance at λ = 280 nm (ϵ_{280} = 5.11 × 10⁴ M⁻¹ cm⁻¹ for holo-FbpA).[26] All spectra were obtained using a CARY 100 Bio UV−vis−NIR spectrophotometer (Varian) at 20.0 °C ± 0.1 °C.

Sulfate Anion Binding to apo-FbpA. Apo-FbpA was dialyzed five times against a buffer of 50 mM MES, 100 mM NaCl at pH 6.5 and diluted with additional fresh buffer to a final concentration of 15 μM. A stock solution of 1.01 M sulfate was prepared from sodium sulfate (Fisher Scientific) in buffer, and adjusted to pH 6.5 with minimal NaOH. Divided quartz cuvettes (Wilmad Labglass) were placed in the sample and reference beam of a CARY 100 Bio UV−Vis−NIR spectrophotometer, with the compartments arranged in series and with each beam passing through a protein and buffer compartment, each of path length = 0.4375 cm. Sulfate was added via a 25-μL microsyringe to the protein compartment of the sample cell and the buffer compartment of the reference cell, incrementally increasing the sulfate concentration from 0.5 to 100 mM. An equivalent volume of buffer was added to the reference protein compartment to correct for dilution. For each sulfate addition, spectra were recorded from 300 to 230 nm at 12 nm/min with 1-nm spectral bandwidth. Difference absorbance spectra were generated by subtracting the spectrum of [SO_4^{2-}] = 0 mM from all scans. Intensities at λ = 238 nm were plotted against sulfate concentration and analyzed by fitting to a nonlinear regression for single-site saturation ligand binding (eq 1) using SigmaPlot 9.0 software

$$\Delta A_{\lambda=238} = \frac{A_{max}[SO_4]}{K_d + [SO_4]} \quad (1)$$

where $\Delta A_{\lambda=238}$ is the change in absorbance at 238 nm on sulfate binding, A_{max} is the maximum absorbance of the curve (when [FbpA]$_{tot}$ = [FbpA-SO₄]), [SO₄] is the molar free sulfate concentration, and K_d is the equilibrium constant for the dissociation of apo-FbpA-SO₄. Identical methodology was used to determine all of the anion binding K_d values listed in Table 1.

Spectroelectrochemistry. Spectroelectrochemistry of FeFbpA-SO₄ was carried out using an in-house anaerobic *o*ptically *t*ransparent *t*hin *l*ayer *e*lectrode (OTTLE) cell with an optical path length of 0.025 ± 0.005 cm, connected to an EG&G Princeton Applied Research

(35) Dhungana, S.; Anderson, D. A.; Mietzner, T. A.; Crumbliss, A. L. *J. Inorg. Biochem.* **2004**, *98*, 1975−1977.

Potentiostat model 263, and CARY 100 Bio UV−vis−NIR spectrophotometer at 20.0 °C ± 0.1 °C as previously described.[25,26] Methyl viologen (MV^{2+}) mediator solution was prepared by dissolving methyl viologen dihydrate (Aldrich) in 0.05 M MES/0.2 KCl, adjusting the pH to 6.5, and diluting to generate a final MV^{2+} concentration of 35 mM. A portion of the MV^{2+} solution was added to the FeFbpA-SO$_4$ in buffer to obtain a 1:7 protein/mediator mol ratio, with a final concentration of ∼0.2−0.7 mM FbpA. All potential values are reported relative to the normal hydrogen electrode (NHE). Spectral scans were performed from 350 to 750 nm, monitoring at $\lambda = 495$ nm for FeFbpA-SO$_4$ and at $\lambda = 391$ and 598 nm for the reduced methyl viologen signal. After each experiment, the OTTLE cell was opened to air to allow reoxidation of the holo-protein, with 85−95% recovery after 12 h.

Determination of Fe^{3+} Binding Constant. A FeFbpA-SO$_4$ stability constant, K'_{eff}, was determined from a competition equilibrium between FeFbpA-SO$_4$ and EDTA at pH 6.5 in 0.05 M MES/0.2 M KCl at 20 °C using methods described previously.[26] The equilibrium position of reaction 2 was monitored spectrophotometrically at the λ_{max} for FeFbpA-SO$_4$ (495 nm) at different protein/EDTA mol ratios from 1:0.5 to 1:5. Aliquots of a 5 mM EDTA (Acros Organics) solution in buffer were added to a FeFbpA-SO$_4$ solution (0.159 mM as determined from the initial absorbance at 280 nm).

$$\text{FeFbpA-SO}_4 + \text{EDTA} \rightleftharpoons \text{FeEDTA} + \text{apo-FbpA-SO}_4 \quad (2)$$

The FeFbpA-SO$_4$ stability constant (K'_{eff}) was calculated using eq 3

$$K = \frac{[\text{FeEDTA}][\text{FbpA-SO}_4]}{[\text{FeFbpA-SO}_4][\text{EDTA}]} = \frac{\beta_{110}^{\text{FeEDTA}}(\text{pH } 6.5)}{K'_{eff}} \quad (3)$$

where K is the experimentally determined equilibrium constant for reaction 2 and $\beta_{110}^{\text{FeEDTA}}$ was calculated at these conditions from known equilibrium constants for the Fe^{3+}/EDTA system[36] by using mass balance equations involving the usual Ringbom's coefficients.[37] The value of K'_{eff} reported is an average of three independent determinations.

Kinetic Measurements by Stopped-Flow Spectrophotometry. The anion-exchange reactions of FeFbpA-SO$_4$ with phosphate and arsenate were studied using an Applied Photophysics stopped-flow (SX.18MV) spectrophotometer equipped with both a photomultiplier and photodiode array detector. All reactions were performed at 25 °C in 0.05 M MES/0.2 M KCl at pH 6.5 under pseudo-first-order conditions with the entering anion at least 10-fold in excess of the protein ([FeFbpA-SO$_4$] = 130 μM). Reactions were monitored in rapid-scan absorbance mode, using the photodiode array detector recording from $\lambda = 350$ to 700 nm to confirm direct conversion from FeFbpA-SO$_4$ ($\lambda_{max} = 495$ nm) to FeFbpA-PO$_4$ ($\lambda_{max} = 481$ nm) or FeFbpA-AsO$_4$ ($\lambda_{max} = 476$ nm) and to determine the wavelengths of the greatest absorbance change in the exchange of FeFbpA-SO$_4$ with phosphate and arsenate ($\lambda = 550$ and 450 nm). Both wavelengths were then used to monitor the change in absorbance as a function of time for each anion at concentrations of 10- to 1000-fold excess over FeFbpA-SO$_4$. Data were analyzed using Applied Photophysics kinetics software.

Structural Analysis of Ligand Binding Sites in FbpA and HitA. Structures for ferric binding proteins FbpA and HitA were obtained from the RCSB Protein Data Bank, http://www.rcsb.org/pdb/Welcome.do. The two pdb files used were 1D9Y, holo-FbpA from *N. gonorrheae*, and 1D9V, apo-HitA from *H. influenzae*.[21,38] The apo form of FbpA has not been deposited into the databank so the apo-form of a homologous protein, HitA, was used to map the iron-free protein interactions. Holo-FbpA and holo-HitA share 71% sequence identity and exhibit identical assembled iron coordination sites.[15]

In order to investigate H-bonding and electrostatics, the pdb files were structurally validated using the MolProbity web service, with three-dimensional (3D) interactive graphics (kinemages) rendered using Prekin, Mage, and Probe, all available at http://kinemage.biochem.duke.edu/.[39,40] The MolProbity web service was used on the pdb files in order to add explicit hydrogens and flip certain amino acids[41] (histidines, asparagines, and glutamines) where it was indicated that such adjustment resulted in an improved structure.[42] "Prekin" was used to generate 3D kinemages from the revised pdb files. "Probe" was then used to generate a pattern of dots representing the van der Waals surface of amino acid residues that are within hydrogen-bonding distances and orientation. The kinemages were rendered in "Mage", and each residue was examined for bonding interactions with phosphate and iron. Figure 1 depicts a cartoon illustration of the kinemages displaying the conserved residues found in FbpA and HitA, and bonding interactions with phosphate and iron.

Calculation of Anion Average Charge (Z_{ave}) and Hydration Enthalpy (ΔH_{hyd}). The average charge of an anion (Z_{ave}) is defined as the sum of the species relative abundance (x_i) multiplied by its charge (Z_i) for all possible species (eq 4).

$$Z_{ave} = \sum x_i Z_i \quad (4)$$

$$Z_i = h - m \quad (5)$$

Z_i is defined in terms of m and h (eq 5), with m equal to the maximum possible charge of an anion (e.g., $m = 3$ for PO$_4^{3-}$) and h equal to the number of bound protons (e.g., $h = 2$ for H$_2$PO$_4^{1-}$). The value of Z_{ave} is dependent on two factors, the anion pK_a values and the solution pH. Rearranging eq 4 to determine x_i in terms of K_a values and pH (as [H$^+$]), Z_{ave} can be calculated by the following eq 6.

$$Z_{ave} = \sum_{h=0}^{m} (h - m) \frac{[\text{H}^+]^{(h)} K_{a_{m-h}} K_{a_{m-(h+1)}} ... K_{a_0}}{\sum_{h=0}^{m} [\text{H}^+]^{(h)} K_{a_{m-h}} K_{a_{m-(h+1)}} ... K_{a_0}} \quad (6)$$

Average charge calculations are used as a way to describe the distribution of anion species as a result of the degree of protonation at pH 6.5.

Z_{ave} values are subsequently used to calculate anion hydration enthalpies (ΔH_{hyd}) according to eq 7

$$\Delta H_{hyd} = \frac{-700 Z_{ave}^2}{r_i + 0.3} \quad (7)$$

where r_i is defined as the thermochemical radius of the anion.[43,44] Calculated ΔH_{hyd} values for sulfate and oxalate anions, where $Z_{ave} = 2.0$, were found to agree with experimental values in the literature.[45,46]

(36) Martell, A. E.; Smith, R. M. *Critical Stability Constants*; Plenum: New York, 1974.

(37) Ringbom, A. *Complexation in Analytical Chemistry: A Guide for the Critical Selection of Analytical Methods Based on Complexation Reactions*; Interscience: New York, 1963.

(38) McRee, D. E.; Bruns, C. M.; Williams, P. A.; Mietzner, T. A.; Nunn, R. Manuscript in preparation.

(39) Lovell, S. C.; Davis, I. W.; Arendall, W. B., III; de Bakker, P. I. W.; Word, J. M.; Prisant, M. G.; Richardson, J. S.; Richardson, D. C. *Proteins: Struc., Funct., Genet.* **2003**, *50*, 437−450.

(40) Davis, I. W.; Murray, L. W.; Richardson, J. S.; Richardson, D. C. *Nucleic Acids Res.* **2004**, *32*, W615−W619.

(41) Even in high-quality structures, approximately 20% of Asn and Gln amide and His imidazole groups are in the wrong orientation and require a 180° flip to optimize H-bonding and/or to avoid clashing of NH$_2$ branches with neighboring atoms. The assignment of NH$_2$ or O branches of amides and N and C of imidazoles is a minor part of protein structure determination and is considered difficult and is, on occasion, not even attempted. However, if a need arises to analyze bound water molecules, H-bonding, or detailed electrostatics, these NH$_2$/O or N/C assignments must be corrected. The MolProbity web service uses small-probe contact dot methodology to analyze van der Waals clashes with H atoms and assigns a score and a visual display which illustrates positive and negative interactions. The user has control to either reject or accept each of the suggested flips.[42]

(42) Word, J. M.; Lovell, S. C.; Richardson, J. S.; Richardson, D. C. *J. Mol. Biol.* **1999**, *285*, 1735−1747.

(43) Smith, D. W. *J. Chem. Educ.* **1977**, *54*, 540−542.

(44) Roobottom, H. K.; Jenkins, H. D. B.; Passmore, J.; Glasser, L. *J. Chem. Educ.* **1999**, *76*, 1570−1573.

(45) Marcus, Y. *Ion Solvation*; Wiley: New York, 1986.

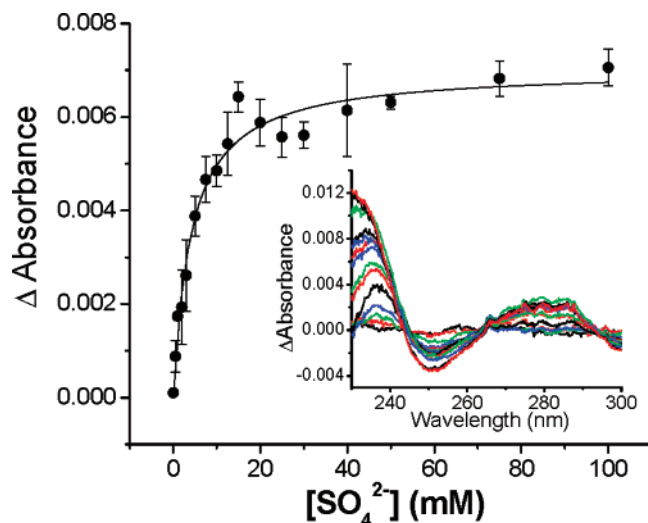(46) Marcus, Y. *Ion Properties*; Marcel Dekker: New York, 1997.

Figure 2. Representative plot for sulfate anion binding to FbpA obtained by difference UV spectroscopy at $\lambda = 238$ nm for apo-FbpA + SO_4^{2-} (difference spectra inset). Solid line represents a fit to a single-site binding model with $K_d = 4.1 \pm 0.5$ mM. Conditions: [apo-FbpA] = 15 μM, [SO_4^{2-}] = 0.5–100 mM in 0.05 M MES/0.1 M NaCl, pH 6.5, 25 °C.

Results

Sulfate Anion Binding to apo-FbpA. Anions are known to bind the apo form of FbpA at the anion binding site while simultaneously preorganizing the iron binding-site tyrosines for Fe^{3+} chelation.[21] UV-difference spectroscopy was used to determine the sulfate anion binding constant for apo-FbpA, expressed below as a dissociation reaction.

$$\text{apo-FbpA-SO}_4 \rightleftharpoons \text{apo-FbpA} + SO_4^{2-} \qquad (8)$$

Representative data are shown in Figure 2, where K_d for reaction 8 is 4.1 mM at pH 6.5, determined by fitting data to eq 1 for single-site binding. Higher-order binding stoichiometries were considered and subsequently rejected due to an inability to fit an equation with differing binding constants to the data, although our method is unable to definitively eliminate the possibility of multiple binding sites of equivalent affinity. However, based on crystallographic evidence for a single phosphate binding to the active site of the apo-protein[21] with a K_d value similar to sulfate (Table 1), the stoichiometry of reaction 8 is considered appropriate. Table 1 is a compilation of sulfate and other anion binding constants for apo-FbpA at pH 6.5.[47] These K_d values vary with the identity of the anion and are in the range observed for other periplasmic anion binding proteins.[20,48–50] The binding of sulfate to FbpA is the weakest observed compared with that of all of the other anions tested.

Thermodynamic Stability of FeFbpA-SO$_4$. As previously observed,[27,35] sulfate anion will satisfy the role of synergistic anion and produce a stable iron–protein assembly, FeFbpA-SO$_4$, with $\lambda_{max} = 495$ nm at pH 6.5. An effective stability constant (K'_{eff}) was determined for the FeFbpA-SO$_4$ assembly by spectrophotometrically monitoring the equilibrium between the protein complex and the competing chelator EDTA (reaction 2). From these data, $K'_{eff} = 1.7 \times 10^{16}$ M^{-1} was calculated for

(47) Vaughan, K. G. Ph.D. Dissertation. University of Pittsburgh, Pittsburgh, PA, 2000.
(48) Luecke, H.; Quiocho, F. A. *Nature* **1990**, *347*, 402–406.
(49) Jacobson, B. L.; Quiocho, F. A. *J. Mol. Biol.* **1988**, *204*, 783–787.
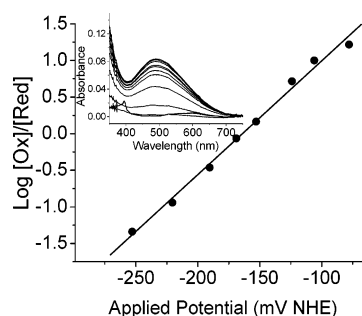(50) Pardee, A. B. *J. Biol. Chem.* **1966**, *241*, 5886–5892.

Figure 3. Representative Nernst plot obtained by spectroelectrochemistry for FeFbpA-SO$_4$ (spectral inset, $\lambda_{max} = 495$ nm). Solid line represents linear least-squares fit to the data where slope and *y*-intercept correspond to Nernstian behavior with single electron transfer ($n = 0.94$) and $E_{1/2} = -158$ mV. Conditions: [Fe^{3+}FbpA-SO$_4$] = 0.7 mM ($\lambda_{max} = 495$ nm), [MV^{2+}] = 4.9 mM ($\lambda_{max} = 391$ and 598 nm) in 0.05 M MES/0.2 M KCl, pH 6.5, 20 °C.

Scheme 1. Range of Reduction Potentials for Fe^{3+} Sequestered by FbpA, with Various Synergistic Anions, FeFbpA-X^a
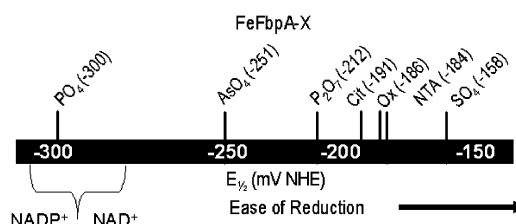

^{a} Data from this work and refs 25 and 26.

equilibrium reaction 9 at pH 6.5, 50 mM MES, in 200 mM KCl at 20 °C. This represents a significant affinity for Fe^{3+} but is the lowest iron affinity of any FeFbpA-X assembly studied to date.[25,26]

$$Fe^{3+}_{aq} + \text{FbpA-SO}_4 \rightleftharpoons \text{FeFbpA-SO}_4 \qquad (9)$$
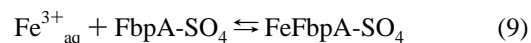
The redox potential of FeFbpA-SO$_4$ was determined by spectroelectrochemistry using an anaerobic OTTLE cell and methyl viologen as a mediator. Well-behaved Nernst plots were obtained (Figure 3) with a slope corresponding to a single electron transfer and intercept, $E_{1/2} = -158$ mV, corresponding to reaction 10

$$Fe^{3+}\text{FbpA-SO}_4 + e^- \rightleftharpoons Fe^{2+}\text{FbpA-SO}_4 \qquad (10)$$
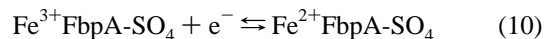
uncorrected for any Fe^{2+} dissociation. This makes FeFbpA-SO$_4$ the most easily reduced of all of the FeFbpA-X assemblies investigated (Scheme 1).[26]

Kinetics of Sulfate Anion Exchange. The kinetics of anion exchange for FeFbpA-SO$_4$ were studied at periplasmic pH (6.5), under pseudo-first-order conditions with the exchanging anions (PO_4^{3-} or AsO_4^{3-}) in excess. The spectral changes observed were consistent with the following exchange reaction, where X = PO_4^{3-} or AsO_4^{3-}.

$$\text{FeFbpA-SO}_4 + X^{n-} \rightarrow \text{FeFbpA-X} + SO_4^{2-} \qquad (11)$$

Kinetic data for both anion-exchange reactions followed a single-exponential decay with a first-order rate constant of k_{obs} = 30 s^{-1} (Figure 4). The observed rate constant for reaction 11 is independent of anion concentration over the range of 10–1000-fold excess over FeFbpA-SO$_4$ (Figure 4 inset).
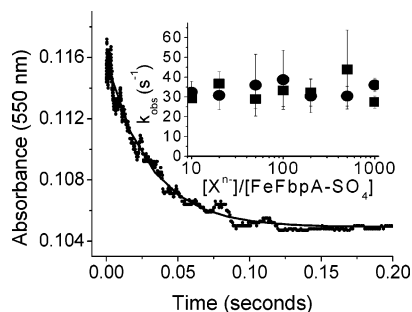
Figure 4. Absorbance change at 550 nm as a function of time for the reaction of FeFbpA-SO$_4$ with PO$_4^{3-}$. Solid line represents a single-exponential decay curve with k_{obs} = 30 s^{-1}. Conditions: [FeFbpA-SO$_4$] = 0.065 mM, [PO$_4^{3-}$] = 0.65 mM, pH = 6.5, in 0.05 M MES/0.2 M KCl at 20 °C. (Inset) Observed first-order rate constant for the reaction of phosphate (squares) and arsenate (circles) with FeFbpA-SO$_4$. Data show no dependence on entering anion identity or concentration and are within one standard deviation of k_{obs} = 30 s^{-1}. Conditions: [FeFbpA-SO$_4$] = 0.065 mM, [X^{n-}] = 0.65−65 mM, pH = 6.5, in 0.05 M MES/0.2 M KCl at 20 °C.

These kinetic data are consistent with the following mechanism

$$\text{FeFbpA-SO}_4 \rightleftharpoons \text{FeFbpA} + \text{SO}_4^{2-} \quad k_1/k_{-1} \qquad (12)$$

$$\text{FeFbpA} + \text{X}^{n-} \rightarrow \text{FeFbpA-X} \quad k_2 \qquad (13)$$

where X^{n-} = PO$_4^{3-}$, AsO$_4^{3-}$. Under pseudo-first-order conditions with excess X^{n-}, the rate law may be expressed as:

$$\text{rate} = \frac{d[\text{FeFbpA-X}]}{dt} = k_{obs}[\text{FeFbpA-SO}_4] \qquad (14)$$

Applying the steady-state assumption to the intermediate FeFbpA, k_{obs} may be expressed as follows:

$$k_{obs} = \frac{k_1 k_2 [\text{X}]}{k_{-1}[\text{SO}_4^{2-}] + k_2[\text{X}]} \qquad (15)$$

At our experimental conditions where [SO$_4^{2-}$] ≪ [X] and making the reasonable assumption that $k_{-1} \approx k_2$, eq 15 reduces to:

$$k_{obs} = k_1 \qquad (16)$$

This is consistent with the observed lack of dependence of k_{obs} on either the identity or concentration of X^{n-} (Figure 4). Consequently, we conclude that the rate constant k_1 for the dissociation of SO$_4^{2-}$ from FeFbpA-SO$_4$ is 30 s^{-1}, and the bound sulfate anion is readily exchanged.

Discussion

Periplasmic Anion Composition and FbpA. The importance of synergistic anion promiscuity in FbpA is exemplified by the modulation of its physicochemical properties by exogenous anions that are both available and otherwise essential to the bacterium. The anion composition of the periplasm is not specifically defined but is rich in diversity.[30] This diverse anion population results from the porin-laced outer membranes of Gram-negative bacteria, through which ions of less than 1000 Da diffuse. The periplasm represents the intervening space between the porous outer membrane and the relatively impervious cytoplasmic membrane. This space is not insignificant, comprising about 30% of the bacterial total volume. It is this

space through which low-molecular weight anionic nutrients must transiently pass from the environment to the cytosol. Proteins such as FbpA and other high-molecular weight molecules such as membrane-derived oligosaccharides, trapped within this space, facilitate the accumulation and uptake of these nutrients.

The anionic composition of the periplasm is complex, dynamic, and heavily influenced by the external environment. Commensal and pathogenic species of the genus *Neisseria* are obligate human parasites and as such are restricted to growth in biological fluids. The phosphate, citrate, and sulfate concentrations within serum are between 0.1 and 1.0 mM[51−53] and therefore are expected to be normal constituents of the low-molecular weight composition of the periplasmic space.

Sulfate as a synergistic anion for Fe^{3+} sequestration by FbpA from *Neisseria* is the focus of this manuscript. There are definitive species of pathogenic bacteria that use inorganic sulfate as a sulfur source, including *N. meningitides*, which can grow using sulfate as a sole source of this nutrient.[54] Most other *Neisseria* strains have been shown to grow with only sulfate or thiosulfate as the lone sulfur source.[54,55] Thus, while our studies are performed in vitro, these experiments are supported by physiological evidence for the accumulation of sulfate within the periplasm, facilitating interaction between this low-molecular weight anion and FbpA.

Synergistic Anion Influence on FeFbpA-X Biophysical Properties. Our physicochemical characterization of FeFbpA-SO$_4$ shows that of all of the iron/FbpA/anion assemblies studied to date,[25,26] the sulfate anion-containing assembly exhibits the lowest binding affinity for Fe^{3+} (log K'_{eff} = 16.2) and the highest $E_{1/2}$ for Fe$^{3+/2+}$ reduction ($E_{1/2}$ = −158 mV). The relative stability of FeFbpA-SO$_4$ reported here is consistent with qualitative results obtained previously by SUPREX methods.[27]

Under our conditions, FeFbpA-SO$_4$ exchange with the biologically important phosphate anion has an ∼20 ms half life, which is consistent with rapid adjustment of the synergistic anion binding with changes in periplasmic conditions. Apparently, the kinetics are controlled by rate-limiting sulfate release, followed by rapid coordination of the entering anion at the iron- and anion binding site. Consequently, FbpA is likely to be responsive to periplasmic anion composition on a kinetic and thermodynamic basis through synergistic anion exchange.

These physicochemical characteristics have significant implications with respect to the possible in vivo mechanisms for periplasm-to-cytosol delivery of the essential nutrient iron. Tight Fe^{3+} binding (K_d = 10$^{-16.2}$ M) in the presence of sulfate ensures delivery of iron to the cytosolic membrane receptor FbpB/FbpC where release to the cytosol could be facilitated by a relatively facile reduction ($E_{1/2}$ = −158 mV). A modulation of this facile reduction can be brought about by anion exchange to form, for example, FeFbpA-PO$_4$, where the $E_{1/2}$ (−300 mV)[26] is less favorable (Scheme 1).

The different synergistic anions have an equivalent influence on the observed range for K'_{eff} and $E_{1/2}$ (∼14 kJ range for both,

(51) Blinn, C. M.; Dibbs, E. R.; Hronowski, L. J. J.; Vokonas, P. S.; Silbert, J. E. *Arthritis Rheum.* **2005**, *52*, 2808−2813.
(52) Politi, L.; Chiaraluce, R.; Consalvi, V.; Cerulli, N.; Scandurra, R. *Clin. Chim. Acta* **1989**, *184*, 155−65.
(53) Patterson, L. A.; DeBlieux, P. M. C. *Emedicine.com* [Online], 2007, http://www.emedicine.com/emerg/topic266.htm (accessed April 2007).
(54) Faou, A. L. *Ann. Microbiol.* (*Paris*) **1984**, *135B*, 3−11.
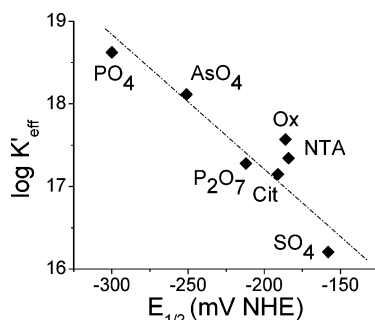(55) Port, J. L.; DeVoe, I. W.; Archibald, F. S. *Can. J. Microbiol.* **1984**, *30*, 1453−1457.

Figure 5. Plot of log of the stability constant (K'_{eff}) for the $Fe^{3+}FbpA$-X assembly as a function of the corresponding $E_{1/2}$ values. The dotted line represents a best fit of a rearranged form of eq 17 with fixed slope of -0.017.

as a function of the synergistic anion). This suggests that the variation in $E_{1/2}$ comes largely from differences in ground-state stabilization of the Fe^{3+} oxidation state in FeFbpA-X. Figure 5 illustrates the trend in log K'_{eff} plotted as a function of $E_{1/2}$ for the various anion-containing forms of FeFbpA-X. The dashed line represents the best fit of a rearranged form of the Nernst equation (eq 17) to the data with the slope of the plot fixed at $-n/58 = -0.017$ mV^{-1}.

$$E_{1/2} = E^o_{aq} + (-0.058/n) \log(K'_{eff}/K^{II}) \qquad (17)$$

Small deviations of the data points from this line most likely represent small fluctuations in the Fe^{2+} binding to FbpA (i.e., K^{II}) and experimental uncertainty.

Structural Analysis of FbpA and Synergistic Anion Interactions. It is important to undertake a careful analysis of the nature of both iron and anion binding by FbpA due to: (1) the requirement of a synergistic anion for tight Fe^{3+} sequestration, (2) the fact that several anions can satisfy this requirement, and (3) the observation that varying the anion identity can modulate several physicochemical characteristics of the FeFbpA-X assembly. For this analysis, it is useful to consider the crystal structures of holo-FbpA-phosphate and apo-HitA-phosphate as models in evaluating the effects of different synergistic anions on the kinetic and thermodynamic stability of FeFbpA-X. In doing this, we note the similar sizes and shapes of phosphate, sulfate, and arsenate. Illustrated in Figure 1A is a simplified version of phosphate anion interactions with the protein–anion binding site and backbone as well as coordination to iron. Phosphate directly interacts with the N-terminus (N-cap) of an α-helix that is adjacent to the iron binding site through the backbone amide of Ala141 and the hydroxyl of Ser139 (both from the C-terminal domain), the iron, and Gln58 from the N-terminal domain of the protein. Glu57 and His9 from the N-terminal domain both bind to the iron. Tyr195 and Tyr196 from the C-terminal domain complete the protein binding complement to iron. In contrast, the bonding network of the apo-protein shown in Figure 1B is simplified and consists of only C-terminal domain interactions with phosphate oriented at a three-point docking site on the N-cap of the aforementioned α-helix where directional hydrogen bonds from the N-cap confer affinity for tetrahedral anions. The location of the binding site of phosphate in both the apo- and holo-FbpA structures is similar to that of the sulfate anion in the periplasmic binding protein, "sulfate binding protein" (SBP)[56] and phosphate (and arsenate) in "phosphate binding protein" (PBP).[57] While SBP and PBP

exhibit selectivity for specific tetrahedral anions, FbpA does not discriminate and will bind sulfate, phosphate, and arsenate.

Several attributes of synergistic anions must be compared in order to determine which contributions are most likely to significantly influence FeFbpA-X ternary assembly stability. One factor in synergistic anion selectivity is shape. Phosphate, arsenate, and sulfate anions are all tetrahedral; thus, FbpA should show no spatial preference between them, as discussed above.

The protonation state of the anion should also be considered as electrostatic interactions appear to play some role in anion selection (cf. K_d values in Table 1). Examining this charge selectivity within anion binding proteins, SBP binds only fully ionized tetrahedral oxydianions (sulfate, selenate, and chromate),[57] while PBP exhibits a preference toward the partially protonated phosphate and arsenate (dibasic and monobasic) species. Hydrogen bond arrays reported for SBP and PBP may provide the key for understanding (1) why FbpA will bind sulfate and phosphate and (2) why sulfate binding to FbpA is weaker in comparison to binding of phosphate or arsenate. Phosphate is held tightly ($K_d = 1 \mu M$) in PBP by twelve strong hydrogen bonds, and sulfate ($K_d = 0.1 \mu M$) is held in SBP by seven.[48,57] Only one residue in PBP (Asp56) is responsible for discriminating between sulfate and phosphate. The fully ionized sulfate dianion is repulsed by the negatively charged PBP-Asp56, whereas either a monobasic ($H_2PO_4^-$) or dibasic (HPO_4^{2-}) phosphate will bind with this hydrogen-bond acceptor.[48] All of the hydrogen-bonding (H-bonding) interactions with sulfate in SBP are with polar residues, and there is no group in the binding site that works as a hydrogen-bond acceptor.

A similar H-bonding activity defines the ability of anions to bind to FbpA at the N-cap of the anion-binding helix, specifically the Ser139 hydroxyl residue. This residue plays a vital role in anion-binding affinity due to rotational degrees of freedom and the ability to donate or accept hydrogen bonds.[48] Elimination of this interaction in FbpA and SBP greatly reduces anion-binding affinity.[58,59] The anion interactions in FbpA are reduced in comparison (Figure 1), and sulfate binding and phosphate binding are weaker than that observed for the SBP and PBP anions (i.e. K_d of apo-FbpA-X on the order of mM) (Table 1). The presence of Glu57 (Figure 1) in FbpA should play a role similar to that of Asp56 in PBP, resulting in discrimination against sulfate. This is not the case (as shown in Figure 1) as a result of (1) a distance of greater than 7 Å between Glu57 and the anion binding site on the other domain of apo-FbpA, (2) the presence of a water molecule between Glu57 and the anion in holo-FbpA, and (3) the presence of Fe^{3+} in holo-FbpA which favorably accepts negative charge from Glu57 through oxygen lone pair donation to a coordinate covalent bond. Although the effect is muted somewhat by the presence of Fe^{3+} and water, the proximity of Glu57 and its negative charge may be the predominate factor in the differences between sulfate and phosphate in FbpA. Mismatched H-bonding pairs such as sulfate and Glu57 have been reported to represent a binding energy barrier of 6–7 kcal/mol.[60] While the interactions shown in Figure 1 for FbpA and discussed for SBP and PBP are structural

(56) Pflugrath, J. W.; Quiocho, F. A. *Nature* **1985**, *314*, 257–260.
(57) Quiocho, F. A. *Curr. Opin. Struct. Biol.* **1991**, *1*, 922–933.
(58) He, J. J.; Quiocho, F. A. *Protein Sci.* **1993**, *2*, 1643–1647.
(59) Adhikari, P.; Weaver, K. D.; Mietzner, T. A. FbpA mutant S139A was found to have reduced Fe^{3+} affinity. Unpublished work, 2007.
(60) Ledvina, P. S.; Yao, N.; Choudhary, A.; Quiocho, F. A. *Proc. Natl. Acad. Sci. U.S.A.* **1996**, *93*, 6786–6791.

in nature,[21,38] they clearly form a platform from which the relative effects of these interactions and their possible origins can be discussed further in the following paragraphs.

In addition to shape and protonation state, a third factor in anion selection is electrostatic field strength. A higher charge density correlates to a more negative hydration enthalpy, such as with sulfate, which results in a stabilization of the primary hydration shell (Table 1). More strongly hydrated ions tend to remain in the bulk solvent. These aspects of synergistic anion interactions with FeFbpA will be discussed further below with the help of extra-thermodynamic relationships. In doing so, it is helpful to break down the analysis of the *variations* in FeFbpA-X stability with differing X^{n-} into the component parts of binding interactions: iron–anion ($Fe^{3+}////X^{n-}$); iron–protein ($Fe^{3+}////FbpA$); and protein–anion ($FbpA///X^{n-}$).

Influence of Iron–Anion, Iron–FbpA, and FbpA–Anion Interactions on the Biophysical Properties of the FeFbpA-X Assembly. The $Fe^{3+}///X^{n-}$ interaction alone is apparently not responsible for the *variations* in FeFbpA-X assembly stability with the identity of X^{n-}. No correlation was observed between log K'_{eff} and pFe, where pFe was taken as a comparative measure of the relative affinity of X^{n-} anions of different denticities for Fe^{3+} (Figure S1, Supporting Information).[61] $Fe^{3+}///X^{n-}$ interaction is evidently not as important as $Fe^{3+}///FbpA$ or $FbpA///X^{n-}$ interactions in determining the observed trends in FeFbpA-X stability.

The protein–anion, $FbpA///X^{n-}$, interactions are reflected in the K_d values measured for various anions bound to apo-FbpA, which span several orders of magnitude (Table 1). In analyzing trends for anion binding to apo-FbpA, Figure 6A illustrates that, while electrostatics play a strong role in determining the variations of FbpA affinity for different anions, the situation is more complicated.[62] This complication is evident in the significant deviation of SO_4^{2-} from the correlation, which may be due to its very negative hydration enthalpy (Table 1). The influence of hydration enthalpy on anion binding to apo-FbpA is illustrated by the trend in Figure 6B, where $\Delta(\Delta G)$ for anion binding ($\Delta(\Delta G_{FbpA-X})$, associated with K_d^{-1})[62] corrected for anion charge (Z_{ave}) is plotted as a function of the anion hydration enthalpy calculated using Z_{ave} at pH 6.5.

In addressing the electrostatic influence on variations in FeFbpA-X assembly stability, we find that combining the influence of both anion charge distribution (Z_{ave}) and protein–anion affinity (K_d) on K'_{eff} provides a useful correlation. This is illustrated in Figure 7, where the relative anion-binding affinity for apo-FbpA is corrected for variations in anion charge (at pH 6.5) by expressing the *x*-axis as $\Delta(\Delta G_{FbpA-X})/Z_{ave}$.[62] This correlation suggests that variations in FeFbpA-X assembly stability are influenced by protein–anion interactions corrected for electrostatics; that is, variations in FeFbpA-X stability correlates with $FbpA///X^{n-}$ interactions due to van der Waals and H-bond interactions. The lack of a correlation between log K'_{eff} and Z_{ave} or log K_d^{-1} (Supporting Information Figure S2A
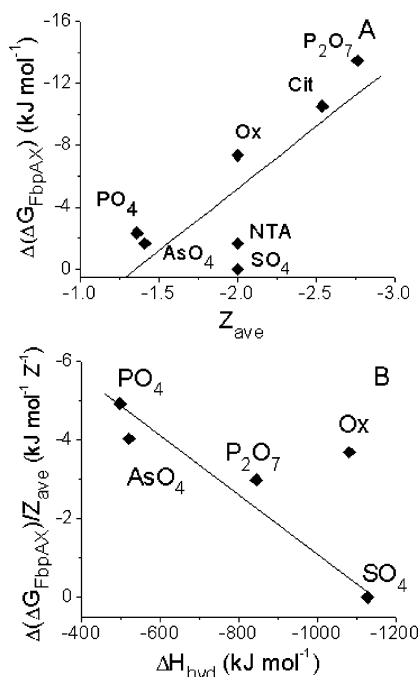

Figure 6. Correlations relating apo-FbpA binding to anions based on anion average charge (Z_{ave}) and hydration enthalpy (ΔH_{hyd}). (A) Plot of $\Delta(\Delta G_{FbpA-X})$ as a function of the average charge on the anion (Z_{ave}), calculated using eq 6. Trend line represents linear least-squares best fit to all data. (B) Plot of apo-FbpA anion binding energy corrected for electrostatic contributions ($\Delta(\Delta G_{FbpA-X})/Z_{ave}$) as a function of the anion hydration enthalpy (ΔH_{hyd}; Table 1). Trend line represents linear least-squares fit to the data, omitting the data point for oxalate for reasons of geometry. $\Delta(\Delta G_{FbpA-X})$ is defined in ref 62.
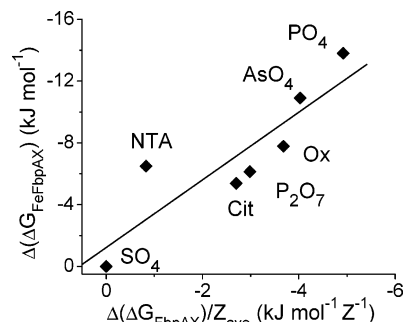

Figure 7. Plot of $\Delta(\Delta G_{FeFbpA-X})$ as a function of anion///apo-FbpA binding corrected for electrostatics ($\Delta(\Delta G_{FbpA-X}/Z_{ave})$). Trend line represents linear least-squares best fit to the data. $\Delta(\Delta G_{FeFbpA-X})$ and $\Delta(\Delta G_{FbpA-X})$ are defined in ref 62.

(61) Raymond, K. N.; Muller, G.; Matzanke, B. F. *Top. Curr. Chem.* **1984**, *123*, 49–102.

(62) The anion-dependent variations in K'_{eff} and K_d are expressed as free energy changes (kJ/mol) relative to FeFbpA-SO4 and apo-FbpA-SO4, respectively. The relative free energy changes for the stability of FeFbpA-X is expressed as $\Delta(\Delta G_{FeFbpA-X})$ and calculated from the difference in log K'_{eff} for FeFbpA-SO4 and the log K'_{eff} for each FeFbpA-X. Similarly, the relative free energy changes for the stability of apo-FbpA-X is expressed as $\Delta(\Delta G_{FbpA-X})$ and calculated from the difference in log K_d for FbpA-SO4 and the log K_d for each apo-FbpA-X.

and S2B) indicates that simple electrostatic binding variations and/or apo-FbpA–anion binding alone are not responsible for the anion identity-dependent fluctuations in K'_{eff}. One factor that may contribute to the observed difference in $\Delta(\Delta G_{FbpA-X})/Z_{ave}$ between phosphate and sulfate (Figure 7) may result from the mismatched H-bond pairing involving Glu57, mentioned above. Figure 8 illustrates that variations in FeFbpA-X assembly stability correlate with calculated anion hydration enthalpy, where data are available.

As a result of this analysis of iron///anion///protein interactions, we can speculate on FbpA binding properties for other anions. Of particular interest is carbonate, the physiological synergistic anion of *h*Tf. While carbonate is able to facilitate stable iron sequestration at the analogous iron binding site in *h*Tf, this anion is unable to bind iron in FbpA at pH 6.5,[26]
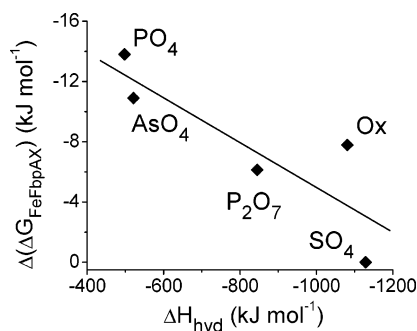
Figure 8. Plot of changes in free energy of the FeFbpA-X complex with different anions ($\Delta(\Delta G_{\text{FeFbpA}-X})$) as a function of anion enthalpy of hydration (ΔH_{hyd}; Table 1). $\Delta(\Delta G_{\text{FeFbpA}-X})$ is defined in ref 62.

although there is evidence that it will bind at higher pH.[28,63] We attribute these observations to the fact that at pH 6.5, carbonate Z_{ave} is -0.6, less negative than at pH 8 and considerably less negative than that for the other anions that function as synergistic anions for FbpA. From the data in Figure 6A, for example, we would predict that apo-FbpA affinity for carbonate at pH 6.5 to be at least an order of magnitude less than for phosphate.

Summary and Conclusions

In conclusion, we have verified the ability of sulfate to act as a synergistic anion to facilitate thermodynamically stable sequestration of Fe^{3+} by FbpA through determination of the FeFbpA-SO$_4$ binding constant and reduction potential. These sulfate anion findings extend the free energy range by which

the synergistic anion can modulate FeFbpA-X complex stability to ~14 kJ ($\Delta(\Delta G_{\text{FeFbpA}-X})$),[62] while also extending the range of anion influence on (Fe^{3+}/Fe^{2+})FbpA-X reduction free energies to ~14 kJ. An examination of the apo-HitA and holo-FbpA crystal structures reveals details of the anion-binding interactions and, with further thermodynamic analysis of the protein assemblies, suggests that the difference in stability of the FeFbpA-X assemblies with varying anions is predominately attributed to the inherent properties of the anion (e.g., ΔH_{hyd}, Z_{ave}), along with the anion−protein interactions. Although variations in K_d for apo-FbpA-X with variation in anion also extend over a ~14 kJ range ($\Delta(\Delta G_{\text{FbpA}-X})$), similar to that noted above for K'_{eff} and $E_{1/2}$, the complexity of these anion interactions, the extent to which they modulate the stability of the FeFbpA-X ternary complex, and their role in the overall delivery of iron in pathogenic bacteria are yet to be fully understood. In conjunction with the diverse composition of the periplasmic space, our observed kinetics of anion exchange and the anion influence on K'_{eff} and $E_{1/2}$ support the hypothesis of redox-facilitated iron delivery to the cytosol, along with the implication of a crucial role for anion identity in FbpA-mediated bacterial iron acquisition.

Supporting Information Available: Two figures. This material is available free of charge via the Internet at http://pubs.acs.org.

(63) Shouldice, S. R.; Skene, R. J.; Dougan, D. R.; McRee, D. E.; Tari, L. W.; Schryvers, A. B. *Biochemistry* **2003**, *42*, 11908−11914.

JA0709268